Anticyclonic suppression of the North Pacific transient eddy activity in midwinter

Satoru Okajima[1], Hisashi Nakamura[1], Yohai Kaspi[2]

[1]Research Center for Advanced Science and Technology, The University of Tokyo, Tokyo, Japan

[2]Department of Earth and Planetary Sciences, Weizmann Institute of Science, Rehovot, Israel

Corresponding author: Satoru Okajima (okajima@atmos.rcast.u-tokyo.ac.jp)

Key Points:

- Anticyclonic contribution is crucial for the midwinter minimum of the North Pacific transient eddy activity
- Anticyclonic suppression is consistent with a midwinter minimum of the net efficiency of energy conversion/generation terms
- More attention should be paid to anticyclones in studying midlatitude storm-track dynamics

Abstract

Dynamical understandings of midlatitude transient eddy activity, especially its midwinter minimum over the North Pacific, are still limited, partly because Eulerian eddy statistics are incapable of separating cyclonic and anticyclonic contributions. Here we evaluate the two contributions separately based on local curvature of instantaneous flow fields to compare their seasonality between the North Pacific and North Atlantic storm-tracks. The anticyclonic contribution is found crucial for the midwinter minimum of the North Pacific transient eddy activity. Eddy energetics reveals that the net efficiency of the anticyclonic contribution in replenishing total transient eddy energy over the North Pacific exhibits a pronounced midwinter minimum, while that of the cyclonic counterpart does not in harmony with precipitation that peaks around midwinter. This study suggests that more attention should be paid to anticyclones in studying midlatitude storm-track dynamics.

Plain Language Summary

Our understanding of the dynamics of midlatitude transient eddy activity, especially its midwinter minimum over the North Pacific, is still limited. This is partly because conventional local statistics based on temporal filtering, which are commonly used as a measure of transient eddy activity, are unable to treat contributions from cyclones and anticyclones separately. Here we evaluate cyclonic and anticyclonic contributions to local eddy statistics separately based on local curvature of instantaneous flow fields, to compare their seasonality between the North Pacific and North Atlantic storm-tracks. The anticyclonic contribution is found crucial for the midwinter minimum of the North Pacific transient eddy activity. We further apply eddy energetics to investigate the relative importance of processes relevant to the maintenance of storm-tracks. The net efficiency of the relevant processes associated with the anticyclonic contribution in replenishing total transient eddy energy over the North Pacific exhibits a pronounced midwinter minimum. By contrast, that of the cyclonic counterpart does not in harmony with precipitation that peaks around midwinter. This study suggests that more attention should be paid to anticyclones in studying midlatitude storm-track dynamics.

1 Introduction

Midlatitude transient eddies that give rise to day-to-day weather variability are one of the rudimentary components of the Earth's climate system (Hurrell, 1995; Shaw et al., 2016). Blackmon (1976) suggested that regions of large band-pass (with periods of 2−6 days) variance of geopotential height correspond to those of frequent cyclone passage over the North Atlantic (NA) and North Pacific (NP) basins, referring to them as "storm-tracks". Those regions are characterized by prominent lower-tropospheric poleward eddy heat flux (Fig. 1) (Blackmon et al., 1977), indicative of baroclinic development of migratory cyclones. Those storm-tracks are collocated with the low-level eddy-driven jets and associated baroclinic zones (Nakamura et al., 2004), and maintained through the effective restoration under the influence of major oceanic frontal zones (Hotta & Nakamura, 2011; Kaspi & Schneider, 2011, 2013).

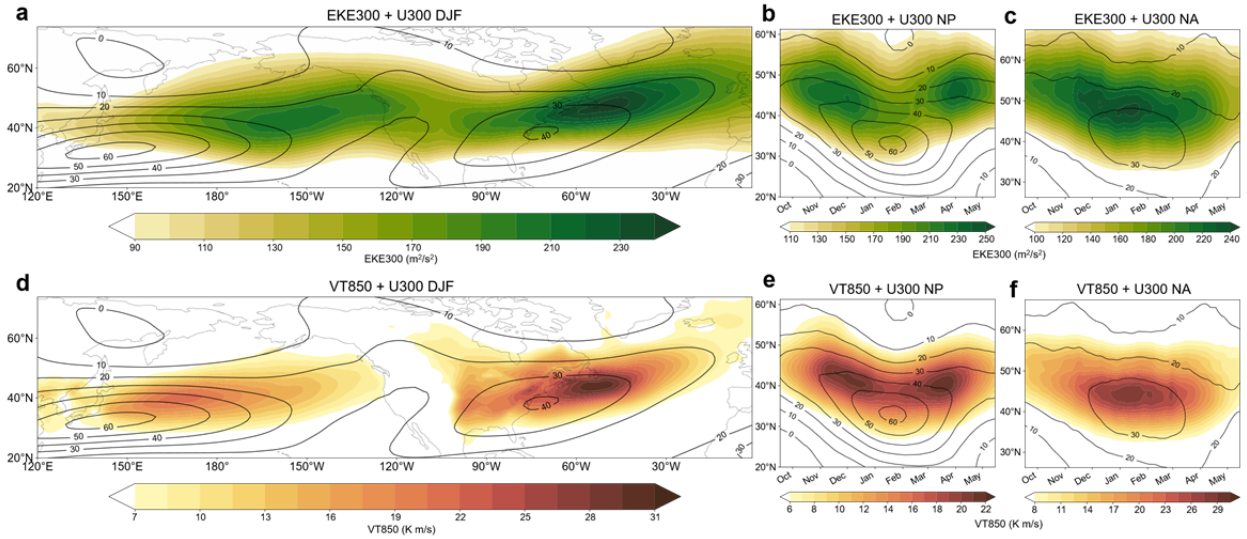

Figure 1. **Wintertime climatological-mean transient eddy activity and its seasonality. a** Climatological-mean wintertime (DJF-mean) EKE_{300} (color, m^2/s^2). Contours denote climatological-mean westerly wind speed (U_{300}; m/s). **b-c** Climatological seasonality in EKE_{300} averaged for 180°−150°W (c) and 60°−30°W (d). Contours denote the corresponding seasonality of U_{300} averaged for 150°E−180° (c) and 70°−40°W (d). A tick mark on the abscissa in b-c represents the first day of a given calendar month. **d-f** Same as in a-c, respectively, but for $V'T'_{850}$ (color, K m/s), averaged over 150°E−180° (e) and 70°−40°W (f).

Eulerian statistics are compatible with quantitative analyses and dynamical diagnostics (Eyring et al., 2021). The eddy energetics is useful for investigating the formation and maintenance mechanisms for the mean westerlies and storm-tracks (Chang et al., 2002; Okajima et al., 2022; hereafter ONK22). Based on Eulerian statistics, the climatological-mean seasonality of storm-track activity, the maintenance mechanisms for the westerly jets and storm-tracks, and their relationship with the lower-boundary condition have been well documented (Chang et al., 2002; Lee & Kim, 2003; Nakamura et al., 2004; Kaspi and Schneider, 2013).

Nevertheless, dynamical understandings of midlatitude transient eddy activity are still limited, especially for the "midwinter minimum (MWM)" or "midwinter suppression" of the NP transient eddy activity (Nakamura, 1992). Under the maximized upper-level jet speed, the climatological-mean NP transient eddy activity exhibits a clear minimum in midwinter as

measured by eddy kinetic energy at 300-hPa (EKE_{300}) (Fig. 1b) and poleward eddy heat transport at 850-hPa ($V'T'_{850}$) (Fig. 1e). This MWM is inconsistent with the baroclinic instability theory (Eady, 1949) and sharply contrasts with the climatological midwinter maximum of the NA transient eddy activity (Figs. 1c and 1f). Various mechanisms have been proposed for this phenomenon, including barotropic (James, 1987) and baroclinic (Schemm & Rivière, 2019) aspects of eddies, diabatic heating (Chang, 2001), trapping of upper-level eddies into the subtropical jet core (Nakamura & Sampe, 2002), an upstream influence (Penny et al., 2010), and structures of the jet streams (Deng & Mak, 2005; Yuval et al., 2018). Based on the comprehensive energetics of transient eddies, ONK22 suggested that multiple processes must be responsible for the MWM. The dynamical origin of the MWM thus remains elusive.

The MWM of the NP transient eddy activity has recently been also investigated through the Lagrangian approach by conducting feature tracking (Schemm & Rivière, 2019; Hadas & Kaspi, 2021). Most of those studies, however, have focused only on migratory cyclones. Okajima et al. (2023; hereafter ONK23) recently revealed that the climatological-mean density of NP surface migratory anticyclones exhibits a clear MWM, while the cyclonic counterpart peaks in midwinter. This suggests that anticyclones are likely key to understanding the mechanisms for the MWM of the NP transient eddy activity. This hypothesis is compatible with the midwinter peak in the climatological-mean precipitation over the NP as well as over the NA (Supplementary Fig. S1), implying that cyclonic activity may not minimize in midwinter even in the NP.

Therefore, whether anticyclones are indeed important for the MWM of the NP transient eddy activity measured by Eulerian eddy statistics needs to be investigated. However, traditional Eulerian eddy statistics are incapable of separating cyclonic and anticyclonic contributions (Wallace et al., 1988). Recently, a novel method to identify three-dimensional regions of individual cyclonic and anticyclonic rotations was proposed (Okajima et al., 2021; hereafter ONK21). The method enables evaluating cyclonic and anticyclonic contributions separately in Eulerian eddy statistics and atmospheric energetics, as a "hybrid" method into which both Eulerian and Lagrangian perspectives are incorporated.

This study thus aims to investigate the seasonality of the cyclonic and anticyclonic contributions to transient eddy activity and energetics within the NP and NA storm-tracks. We will demonstrate that anticyclones are more important for the MWM of the NP transient eddy activity, to argue that more attention should be paid to migratory anticyclones in studying midlatitude storm-track dynamics.

2 Data and Methods

2.1 Atmospheric reanalysis

We analyze 6-hourly global fields of atmospheric variables, including geopotential height, air temperature, wind velocity, and diabatic heating rates in pressure coordinates, in addition to sea-level pressure, obtained from the Japanese 55-year atmospheric reanalysis (JRA-55) by the Japan Meteorological Agency (JMA) (Kobayashi et al., 2015; Harada et al., 2016) for the period 1958-2022. Variables at selected pressure levels are available on a 1.25°×1.25° grid. At each grid point, fluctuations of a given variable with synoptic-scale transient eddies have been extracted locally from the 6-hourly reanalysis data as its deviations from their low-pass-filtered

fields through a 121-point Lanczos filter with a cutoff period of 8 days. Plots showing seasonal evolutions (as in Fig. 1) are produced after applying a 31-day running mean to daily climatology.

2.2 Cyclonic and anticyclonic contributions to Eulerian eddy statistics

Climatological-mean eddy Eulerian statistics are calculated separately for cyclonic and anticyclonic contributions based on two-dimensional local flow curvature κ_2 (ONK21). It is calculated at a given vertical level instantaneously from horizontal winds as

$$\kappa_2 \equiv \frac{1}{R_S} = \frac{1}{V^3}\left(-uvu_x + u^2v_x - v^2u_y + uvv_y\right),$$

where R_S denotes the curvature radius, V scaler wind speed, and a subscript denotes zonal or meridional derivative, respectively. A positive (negative) value signifies a cyclonic (anticyclonic) rotation in the Northern Hemisphere. This method effectively removes the effect of shear vorticity, associated with the strong westerlies and requires no temporal filtering to determine the shape of the regions of rotations. We use unfiltered winds to calculate curvature as in ONK23, who conducted tracking of surface migratory cyclones and anticyclones based on unfiltered SLP. It also helps to retain asymmetry between cyclonic and anticyclonic rotations (e.g., gradient wind balance).

Separate contributions from cyclonic and anticyclonic regions to Eulerian statistics are evaluated by accumulating instantaneous contributions only at grid points where cyclonic or anticyclonic curvature is observed (ONK21), as a practical, *ad hoc* method. In this study, the threshold curvatures for cyclonic and anticyclonic rotations are $\pm 3.3\times10^{-6}$ m^{-1}, respectively, which are equivalent to a curvature radius of ~3,000km. It aims to practically remove the effect of planetary-scale waves, which are regarded as part of a background flow for transient eddies. Nevertheless, we have confirmed that results are qualitatively similar when a zero curvature threshold is used (Supplementary Fig. S2) or the effect of background planetary-scale waves is eliminated by spectral truncation (subtracting T4 winds from the total winds while calculating curvature) (Supplementary Fig. S3).

2.3 Energetics

The formulation of energetics associated with transient eddy activity follows ONK22. To assess the relative importance of relevant processes independent of eddy amplitude, energy conversion/generation rates are normalized by the total eddy energy as the sum of EKE and EAPE (eddy available potential energy), which is not separated into cyclonic and anticyclonic contributions. The normalized rates are referred to as "*efficiencies*" (Kosaka & Nakamura, 2010; ONK22). The zonally-asymmetric climatological-mean state is considered as a background state for high-pass-filtered fluctuations. All the terms related to eddy energy and energy conversion/generation rates are three-dimensionally integrated over the NP [130°E−130°W, 20°−65°N] or NA [80°−10°W, 25°−65°N] domain and from the surface to the 100-hPa level. In this study, energy conversion rates from low-frequency variability to sub-weekly eddies are neglected, because they are only of secondary importance (ONK22).

3 Results

3.1 Probability of cyclonic and anticyclonic regions

In the wintertime (DJF-mean) upper troposphere (Fig. 2a), cyclonic regions are more frequently observed north of the jet core region over each of the ocean basins. By contrast, anticyclonic regions are more frequent downstream of a jet core region. Note that those cyclonic and anticyclonic regions are identified through local curvature free from shear vorticity of a jetstream. The spatially contrasting probability of cyclonic and anticyclonic regions is common to the two major storm-tracks. In the lower troposphere (Fig. 2b), cyclonic regions are more frequent along a low-level eddy-driven jet axis as well as to its north, consistent with results based on cyclone tracking (Hoskins & Hodges, 2002; Shaw et al., 2016; ONK23).

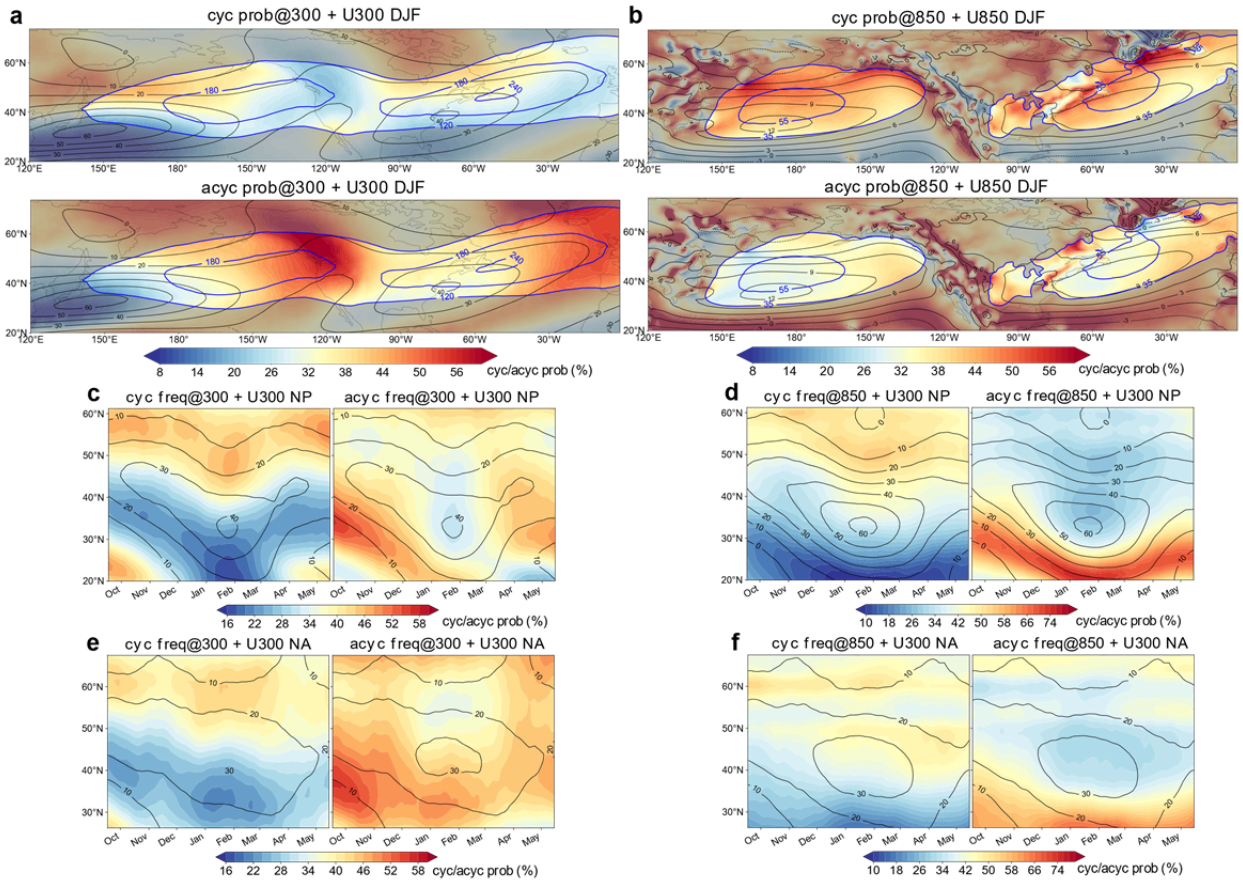

Figure 2. **Climatological-mean probability of cyclonic/anticyclonic regions and its seasonality. a-b** Climatological-mean wintertime (DJF) distributions of probability of cyclonic (upper) and anticyclonic (lower) regions (color, %) at 300-hPa (a) and 850-hPa (b). Black contours denote climatological-mean U_{300} (a) and U_{850} (b) (m/s). Blue contours signify climatological-mean EKE at 300 hPa (a) and 850 hPa (b) (m^2/s^2). **c** Climatological seasonality in probability of cyclonic (left) and anticyclonic (right) regions (color, %) at 300-hPa averaged for 180°−150°W. Contours denote the corresponding seasonality of U_{300} averaged for 180°−150°W. **d** Same as in c, but for probability of cyclonic and anticyclonic regions at 850-hPa and U_{300}

averaged for 150°E−180°. **e-f** Same as in c-d, respectively, but for probability of regions and U_{300} averaged for 70°−40°W (e) and 60°−30°W (f).

The climatological seasonality of the probability of lower-tropospheric cyclonic and anticyclonic regions (Fig. 2d) is consistent with the results based on tracking of NP surface migratory cyclones and anticyclones, respectively (ONK23). Over the midwinter NP, the probability of lower-tropospheric cyclonic region peaks, and its maximum expands equatorward under the strongest, equatorward-shifted Pacific jet. Contrastingly, the anticyclonic counterpart minimizes in midwinter around the storm-track axis near 40°N. The corresponding probability of upper-tropospheric cyclonic curvature exhibits a similar midwinter maximum and equatorward expansion (Fig. 2c). In comparison, over the NA, lower- and upper-tropospheric cyclonic regions exhibit less obvious seasonality than over the NP, as the NA jet exhibits only modest equatorward displacement and strengthening in midwinter (Figs. 2e-f).

3.2 Cyclonic and anticyclonic contributions to transient eddy activity

Figures 3a-d show the climatological seasonality of cyclonic and anticyclonic contributions to upper-tropospheric transient eddy activity over the NP and NA, where the latter contribution is overall greater than the former. The anticyclonic contribution to EKE_{300} exhibits a pronounced MWM under the strong NP jet (Fig. 3a), while the cyclonic counterpart does not minimize in midwinter (Fig. 3b). The distinct seasonality suggests that the anticyclonic contribution is predominantly responsible for the MWM of the total EKE_{300} (Fig. 1b). In contrast to the NP, the anticyclonic contribution to EKE_{300} over the NA does not exhibit a clear MWM (Fig. 3c). The cyclonic counterpart maximizes in midwinter (Fig. 3d). Their contributions correspond to the single peak in EKE_{300} over the NA (Fig. 1c).

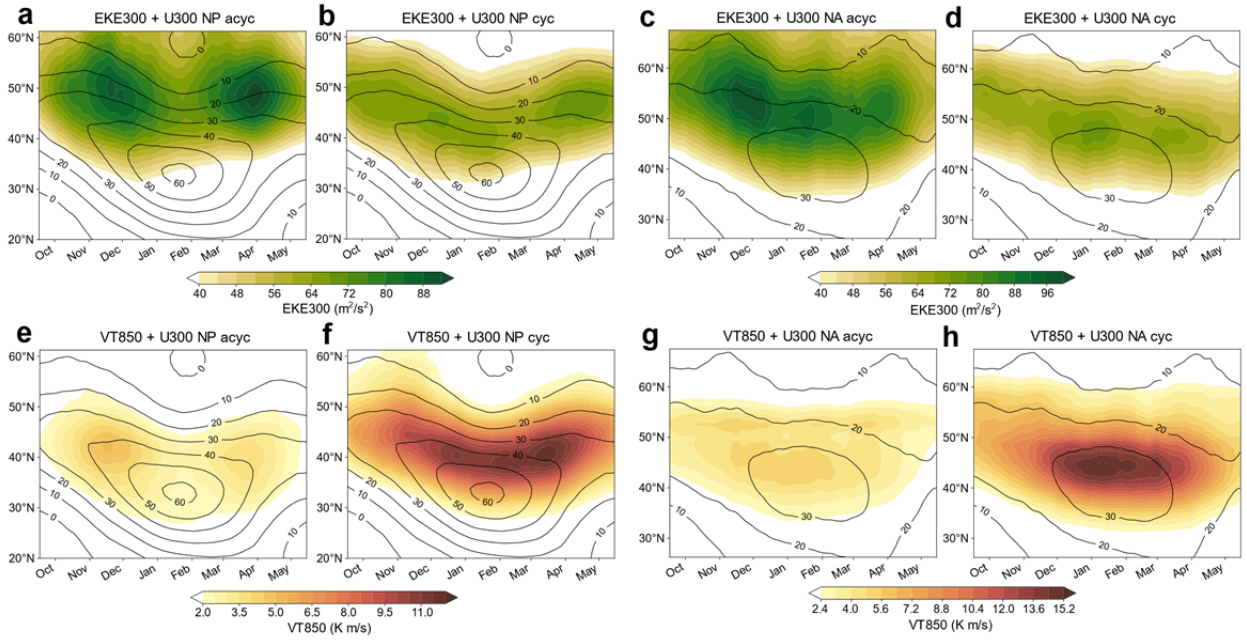

Figure 3. **Seasonality of anticyclonic and cyclonic contributions to transient eddy activity**. **a-b** Climatological seasonality in EKE_{300} reconstructed only with anticyclonic (a) and cyclonic

(b) regions averaged for 180°−150°W. Contours denote the corresponding seasonality of climatological-mean U_{300} averaged for 150°E−180°. **c-d** Same as in a-b, respectively, but for EKE_{300} averaged for 60°−30°W. Contours denote the corresponding seasonality of climatological-mean U_{300} averaged for 70°−40°W. **e-h** Same as in a-d, respectively, but for $V'T'_{850}$ averaged for 150°E−180° (e-f) and 70°−40°W (g-h).

The climatological seasonality of cyclonic and anticyclonic contributions to $V'T'_{850}$ also exhibits discernible differences between the NP and NA (Figs. 3e-h), similar to those of EKE_{300}. Although the anticyclonic contribution to $V'T'_{850}$ is overall substantially weaker (<50%) than the cyclonic counterpart as shown by ONK21, only the former exhibits an obvious MWM over the NP as the total $V'T'_{850}$ does (Figs. 3e and 1e). By contrast, the cyclonic contribution to $V'T'_{850}$ is rather constant throughout the winter with a slight peak in late winter (Fig. 3f). This is compatible with the midwinter peak in precipitation over the NP associated with cyclonic regions (Supplementary Figs. S4). Contrastingly, over the NA, both the cyclonic and anticyclonic contributions to $V'T'_{850}$ exhibit no clear MWM (Figs. 3f and 3h), contributing to the single midwinter peak in the total $V'T'_{850}$ (Fig. 1f).

3.3 Energetics

Quantitative evaluation of eddy energetics separately for the cyclonic and anticyclonic contributions delineates relevant processes for their distinct seasonality. We evaluate the "efficiency" of a given energetic term, whose reciprocal represents the time to replenish the three-dimensionally integrated total eddy energy (EKE_{3D}+$EAPE_{3D}$) over each of the entire NP and NA storm-track regions solely by that term, which is independent of the eddy amplitude (ONK22).

Over the NP (Fig. 4a), a more distinct MWM is observed for the anticyclonic contribution than for the cyclonic counterpart to each of EKE_{3D}, $EAPE_{3D}$, and EKE_{3D}+$EAPE_{3D}$, which is consistent with the preceding results (Fig. 3). Over the NA (Fig. 4d), contrastingly, those three types of eddy energy all peak in early- or mid-winter, regardless of the cyclonic or anticyclonic contribution. For both the NP and NA, the systematically larger cyclonic $EAPE_{3D}$ compared to its anticyclonic counterpart may be an indication of the more baroclinic nature of migratory cyclones.

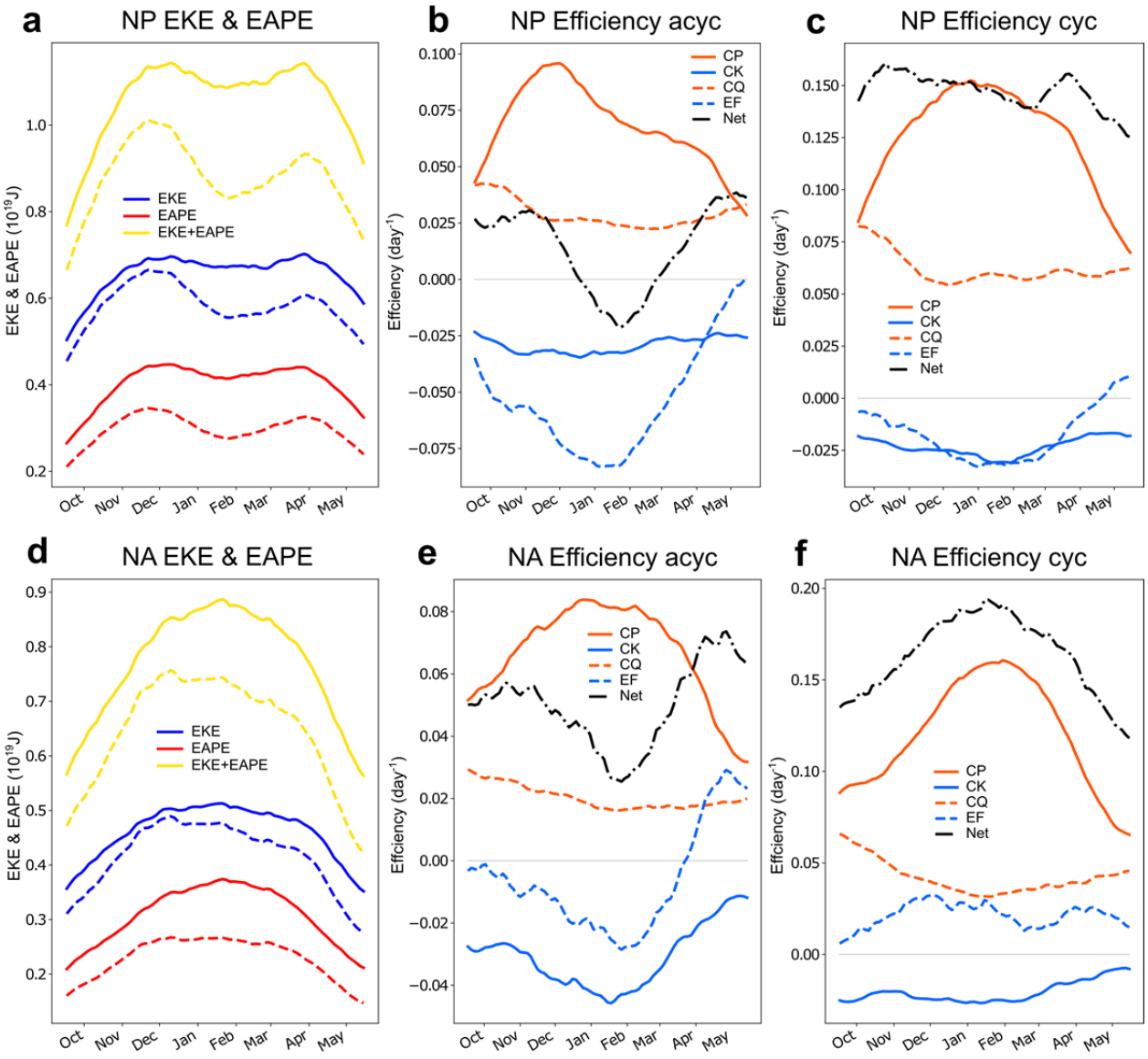

Figure 4. **Seasonality in the energetics regarding the anticyclonic and cyclonic contributions**. **a** Climatological-mean seasonal evolution of EKE_{3D} (blue), $EAPE_{3D}$ (red), and EKE_{3D}+$EAPE_{3D}$ (yellow) (10^{19}J). All the quantities plotted are integrated three-dimensionally over the NP. Solid and dashed lines signify the cyclonic and anticyclonic contributions, respectively. **b-c** Same as in a, but for "efficiency" (day^{-1}) of barotropic energy conversion (CK; blue), baroclinic energy conversion (CP; red), energy generation through diabatic processes (CQ; dashed red), and horizontal energy flux term (EF; dashed blue) contributed to by anticyclonic (b) and cyclonic regions (c) over the NP. Black dash-dotted lines denote the net efficiency relevant to the budget of EKE_{3D}+$EAPE_{3D}$ (viz. CK+CP+CQ+EF). **d-f** Same as in a-c, respectively, but for the NA.

The net "efficiency" of the energy conversion/generation terms associated with anticyclonic regions exhibits a distinct MWM over the NP (Fig. 4b). This is contributed to mainly by the declining positive efficiency of the baroclinic energy conversion (CP) from early winter and the reducing negative efficiency of the net energy flux term (EF) into spring. This

seasonality of the anticyclonic EF term is mainly due to the energy outflux through the eastern boundary and the energy influx through the western boundary (Supplementary Fig. S5a), the latter of which corresponds to the seeding effect from upstream (Penny et al., 2010). By contrast, the net efficiency associated with cyclonic regions over the NP exhibits only a slight minimum in early March (Fig. 4c), while systematically higher than its anticyclonic counterpart throughout the cold season. Among the cyclonic contributions evaluated, the CP term exhibits the highest efficiency with the most pronounced peak in midwinter.

The anticyclonic contribution to the net efficiency of energy conversion/generation exhibits a well-defined MWM also over the NA (Fig. 4e). This is primarily due to the barotropic energy conversion (CK) and EF terms, whose negative contribution maximizes in midwinter, acting against the midwinter maximum of the CP efficiency. In midwinter, the energy outflux maximizes, while the energy influx from the upstream minimizes (Supplementary Fig. S5b). In comparison, the net efficiency associated with cyclonic regions exhibits a sharp midwinter maximum over the NA (Fig. 4f), due primarily to the pronounced midwinter maximum in the CP efficiency. Unlike its anticyclonic counterpart, the cyclonic EF term is positive and does not minimize in midwinter (Fig. 4f). In essence, both the less distinct MWM of the anticyclonic net efficiency, and the more prominent midwinter maximum of the cyclonic counterpart, correspond to the midwinter peak in the NA eddy activity (Figs. 1e-f).

For both the NP and NA, the efficiency of the total diabatic energy generation (CQ) is positive throughout the cold season with a slight MWM over the NA (Figs. 4b-c and 4e-f). This is due to a midwinter offset between the maximized generation through precipitation and maximized damping through air-sea heat exchange represented as the vertical diffusion term (Supplementary Figs. S5c-d). This offset is more evident in the cyclonic contribution.

4 Conclusions

Utilizing a novel method for separate identification of cyclonic and anticyclonic regions with local flow curvature (ONK21), this study demonstrates that the anticyclonic contribution to transient eddy activity plays a pivotal role in setting its MWM over the NP. We thus posit that not only cyclones but also anticyclones need to be considered in investigating transient eddy activity measured as Eulerian eddy statistics, which has been ignored in previous studies. The importance of anticyclones is compatible with the fact that the MWM of the NP transient eddy activity has been reproduced in Eulerian statistics even in coarse-resolution GCMs (Christoph et al., 1997; Zhang & Held, 1999).

For the contrasting seasonality of cyclonic and anticyclonic contributions to transient eddy activity, their probability is also found important (Fig. 2). We, therefore, hypothesize that the MWM of surface migratory anticyclone density over the NP (ONK23) is one of the crucial factors for the MWM of transient eddy activity. Figure 5 schematically depicts factors giving rise to the MWM of transient eddy activity over the NP, based on the results in this study in combination with the distinct seasonality of NP surface migratory cyclones and anticyclones (ONK23). An important factor, which is unique to the NP storm-track, is midwinter suppression of the genesis of migratory surface anticyclones around the Japan Sea under the intensified

monsoonal northwesterlies and southward-shifted upper-level jet (ONK23). Another factor is the midwinter maximum of the eddy energy outflux from the eastern NP associated mainly with anticyclonic regions. The tendency of migratory anticyclones to propagate farther downstream compared to cyclones that exhibit a poleward-propagating tendency away from the jet because of diabatic heating (Tamarin & Kaspi, 2016; Tamarin & Kaspi, 2017) may also be relevant.

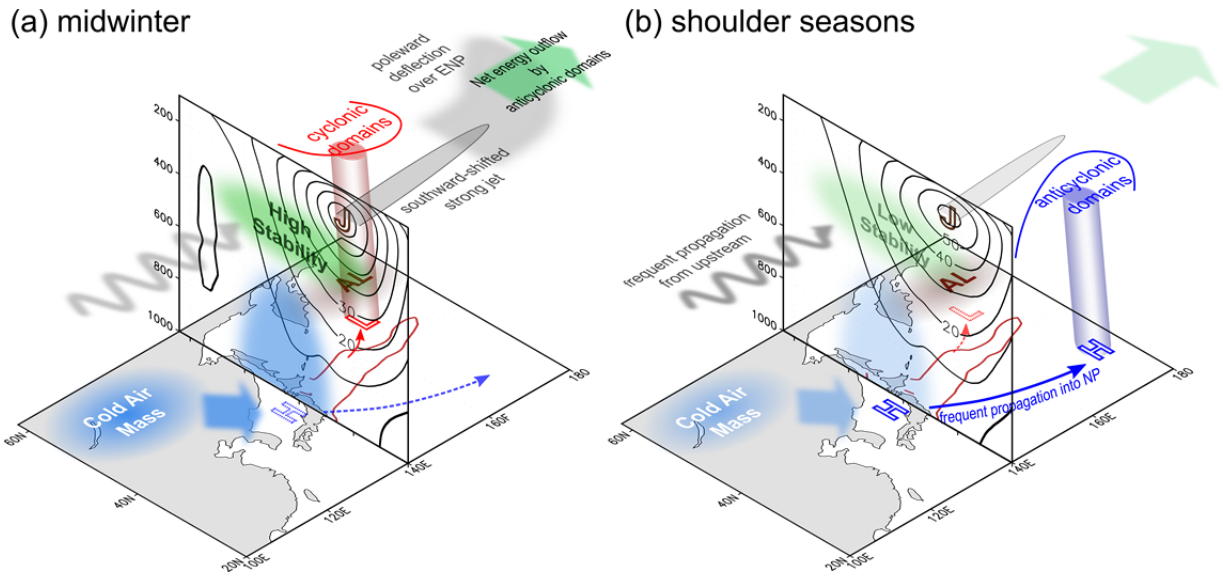

Figure 5. Schematic of seasonality of the North Pacific transient eddy activity. Climatological-mean situations in (a) midwinter and (b) shoulder seasons. Black contours on vertical sections indicate climatological-mean westerly wind speed (m/s) averaged for 130°−140°E in (a) midwinter (around 24Jan) and (b) early spring (around 19Mar).

The seasonality of the net efficiency is still asymmetric between the cyclonic and anticyclonic contributions even after normalized by their probability over the NP and NA (Supplementary Fig. S6). This suggests that intrinsic cyclone-anticyclone asymmetry may exist regardless of their probability. An intriguing finding is that the net efficiency only of the anticyclonic energy conversion/generation terms exhibits a distinct MWM both over the NP and NA. Potentially relevant factors regarding the asymmetry include diabatic heating, gradient wind balance, and typical moving direction, which will be covered by our future studies.

How the contrasting cyclonic and anticyclonic contributions lead to the MWM as their net effect is yet to be understood. Applying the framework used in this study to idealized GCM experiments with zonally-symmetric configurations (as by Novak et al., 2020; Yuval et al., 2018) will be informative. The MWM of the NA transient eddy activity under the extremely strong jet years (Afargan & Kaspi, 2017; Montoya Duque et al., 2021) may also be relevant for understanding the mechanism.

Finally, this study suggests that we should consider an anticyclonic contribution in investigating transient eddy activity in the warmed future climate (Eyring et al., 2021; Seneviratne et al., 2021), in which the westerly jet is overall projected to shift or expand poleward. Such investigations have been carried out either by Eulerian eddy statistics (Harvey et

316 al., 2020) or by cyclone tracking (Priestley & Catto, 2022). The "hybrid" perspective would be
317 helpful for a deeper understanding of future changes in storm-track activity.

318

319 **Acknowledgments**

320 This study is supported in part by the Japanese Ministry of Education, Culture, Sports, Science
321 and Technology (MEXT) through the Arctic Challenge for Sustainability II (ArCS-II;
322 JPMXD1420318865) and through the advanced studies of climate change projection (SENTAN;
323 JPMXD0722680395, by the Japan Science and Technology Agency through COI-NEXT
324 JPMJPF2013, by the Japanese Ministry of Environment through Environment Research and
325 Technology Development Fund JPMEERF20222002, and by the Japan Society for the
326 Promotion of Science (JSPS) through Grants-in-Aid for Scientific Research 19H05702 (on
327 Innovative Areas 6102), 20H01970, 22H01292, and 22K14097. Y.K. acknowledges support
328 from the JSPS Invitational Fellowship for Research in Japan that supported a sabbatical at the
329 University of Tokyo and ignited this collaboration, for support from the Research Center for
330 Advanced Technology and Science at the University of Tokyo and the Israeli Science
331 Foundation (grant 996/20).

332

333 **Open Research**

334 The JRA-55 reanalysis is available online at https://jra.kishou.go.jp/JRA-55/index_en.html. The
335 GPCP v3.2 monthly precipitation data is available online at
336 https://disc.gsfc.nasa.gov/datasets/GPCPMON_3.2/summary?keywords=GPCPMON. Inkscape
337 v1.0.1 (https://inkscape.org/) is used to generate the figures.

338

References

Afargan, H., & Kaspi, Y. (2017). A midwinter minimum in North Atlantic storm track intensity in years of a strong jet. *Geophysical Research Letters*, 44(24), 12–511

Blackmon, M. L. (1976). A climatological spectral study of the 500 mb geopotential height of the Northern Hemisphere. *Journal of the Atmospheric Sciences*, 33(8), 1607–1623.

Blackmon, M. L., Wallace, J. M., Lau, N.-C., & Mullen, S. L. (1977). An Observational Study of the Northern Hemisphere Wintertime Circulation. *Journal of the Atmospheric Sciences*, 34(7), 1040–1053.

Chang, E. K. M. (2001). GCM and Observational Diagnoses of the Seasonal and Interannual Variations of the Pacific Storm Track during the Cool Season. *Journal of the Atmospheric Sciences*, 58(13), 1784–1800.

Chang, E. K. M., Lee, S., & Swanson, K. L. (2002). Storm track dynamics. *Journal of Climate*, 15(16), 2163–2183.

Christoph, M., Ulbrich, U., & Speth, P. (1997). Midwinter suppression of North Hemisphere storm track activity in the real atmosphere and in GCM experiments. *Journal of the Atmospheric Sciences*, 54(12), 1589–1599.

Deng, Y., & Mak, M. (2005). An Idealized Model Study Relevant to the Dynamics of the Midwinter Minimum of the Pacific Storm Track. *Journal of the Atmospheric Sciences*, 62(4), 1209–1225.

Eady, E. T. (1949). Long Waves and Cyclone Waves. *Tellus*, 1(3), 33–52.

Eyring, V., Gillett, N. P., Achutarao, K., Barimalala, R., Barreiro Parrillo, M., Bellouin, N., et al. (2021). Human Influence on the Climate System. *Climate Change 2021: The Physical Science Basis. Contribution of Working Group I to the Sixth Assessment Report of the Intergovernmental*

Panel on Climate Change. V. Masson-Delmotte, P. Zhai, A. Pirani, S. L. Connors, C. Péan, S. Berger, et al., Eds. Pp. 423−552, Cambridge Univ. Press.

Hadas, O., & Kaspi, Y. (2021). Suppression of Baroclinic Eddies by Strong Jets. *Journal of the Atmospheric Sciences, 78(8)*, 2445–2457.

Harada, Y., Kamahori, H., Kobayashi, C., Endo, H., Kobayashi, S., Ota, Y., et al. (2016). The JRA-55 Reanalysis: Representation of Atmospheric Circulation and Climate Variability. *Journal of the Meteorological Society of Japan*, 94(3), 269–302.

Harvey, B. J., Cook, P., Shaffrey, L. C., & Schiemann, R. (2020). The response of the northern hemisphere storm tracks and jet streams to climate change in the CMIP3, CMIP5, and CMIP6 climate models. *Journal of Geophysical Research*, 125(23), e2020JD032701.

Hoskins, B. J., & Hodges, K. I. (2002). New Perspectives on the Northern Hemisphere Winter Storm Tracks. *Journal of the Atmospheric Sciences*, 59(6), 1041–1061.

Hotta, D., & Nakamura, H. (2011). On the Significance of the Sensible Heat Supply from the Ocean in the Maintenance of the Mean Baroclinicity along Storm Tracks. *Journal of Climate*, 24(13), 3377–3401.

Hurrell, J. W. (1995). Transient Eddy Forcing of the Rotational Flow during Northern Winter. *Journal of the Atmospheric Sciences*, 52(12), 2286–2301.

James, I. N. (1987). Suppression of baroclinic instability in horizontally sheared flows. J*ournal of the Atmospheric Sciences*, 44(24), 3710–3720.

Kaspi, Y., & Schneider, T. (2011). Winter cold of eastern continental boundaries induced by warm ocean waters. *Nature*, 471(7340), 621–624.

Kaspi, Y., & Schneider, T. (2013). The Role of Stationary Eddies in Shaping Midlatitude Storm Tracks. *Journal of the Atmospheric Sciences*, 70(8), 2596–2613.

Kobayashi, S., Ota, Y., Harada, Y., Ebita, A., Moriya, M., Onoda, H., et al. (2015). The JRA-55 Reanalysis: General Specifications and Basic Characteristics. *Journal of the Meteorological Society of Japan*, 93(1), 5–48.

Kosaka, Y., & Nakamura, H. (2010). Mechanisms of Meridional Teleconnection Observed between a Summer Monsoon System and a Subtropical Anticyclone. Part I: The Pacific–Japan Pattern. *Journal of Climate*, 23(19), 5085–5108.

Lee, S., & Kim, H.-K. (2003). The Dynamical Relationship between Subtropical and Eddy-Driven Jets. *Journal of the Atmospheric Sciences*, 60(12), 1490–1503.

Montoya Duque, E., Lunkeit, F., & Blender, R. (2021). North Atlantic midwinter storm track suppression and the European weather response in ERA5 reanalysis. *Theoretical and Applied Climatology*, 144(3), 839–845.

Nakamura, H. (1992). Midwinter Suppression of Baroclinic Wave Activity in the Pacific. *Journal of the Atmospheric Sciences*, 49(17), 1629–1642.

Nakamura, H., & Sampe, T. (2002). Trapping of synoptic-scale disturbances into the North-Pacific subtropical jet core in midwinter. *Geophysical Research Letters*, 29(16), 1–4.

Nakamura, H., Sampe, T., Tanimoto, Y., & Shimpo, A. (2004). Observed associations among storm tracks, jet streams and midlatitude oceanic fronts. Earth's Climate: The Ocean–Atmosphere Interaction, *Geophys. Monogr*, 147, 329–345.

Novak, L., Schneider, T., & Ait-Chaalal, F. (2020). Midwinter Suppression of Storm Tracks in an Idealized Zonally Symmetric Setting. *Journal of the Atmospheric Sciences*, 77(1), 297–313.

Okajima, S., Nakamura, H., & Kaspi, Y. (2021). Cyclonic and anticyclonic contributions to atmospheric energetics. *Scientific Reports*, 11(1), 13202.

Okajima, S., Nakamura, H., & Kaspi, Y. (2022). Energetics of transient eddies related to the midwinter minimum of the North Pacific storm-track activity. *Journal of Climate*, 35(4), 1137–1156.

Okajima, S., Nakamura, H., & Kaspi, Y. (2023). Distinct roles of cyclones and anticyclones in setting the midwinter minimum of the North Pacific eddy activity: a Lagrangian perspective. *Journal of Climate*, 36(14), 4793–4814.

Penny, S., Roe, G. H., & Battisti, D. S. (2010). The Source of the Midwinter Suppression in Storminess over the North Pacific. *Journal of Climate*, 23(3), 634–648.

Priestley, M. D. K., & Catto, J. L. (2022). Future changes in the extratropical storm tracks and cyclone intensity, wind speed, and structure. *Weather and Climate Dynamics*, 3(1), 337–360.

Schemm, S., & Rivière, G. (2019). On the Efficiency of Baroclinic Eddy Growth and How It Reduces the North Pacific Storm-Track Intensity in Midwinter. *Journal of Climate*, 32(23), 8373–8398.

Seneviratne, S. I., Zhang, X., Adnan, M., Badi, W., Dereczynski, C., Di Luca, A., et al. (2021). Weather and climate extreme events in a changing climate. *Climate change 2021: The physical science basis. Contribution of working group I to the sixth assessment report of the intergovernmental panel on climate change* (pp. 1513–1766). V. Masson-Delmotte, P. Zhai, A. Pirani, S. L. Connors, C. Péan, S. Berger, et al. (Eds.), Cambridge University Press.

Shaw, T. A., Baldwin, M., Barnes, E. A., Caballero, R., Garfinkel, C. I., Hwang, Y.-T., et al. (2016). Storm track processes and the opposing influences of climate change. *Nature Geoscience*, 9(9), 656–664.

Tamarin, T., & Kaspi, Y. (2016). The Poleward Motion of Extratropical Cyclones from a Potential Vorticity Tendency Analysis. *Journal of the Atmospheric Sciences*, 73(4), 1687–1707.

Tamarin, T., & Kaspi, Y. (2017). The poleward shift of storm tracks under global warming: A Lagrangian perspective. *Geophysical Research Letters*, 44(20), 10666–10674.

Wallace, J. M., Lim, G.-H., & Blackmon, M. L. (1988). Relationship between Cyclone Tracks, Anticyclone Tracks and Baroclinic Waveguides. *Journal of the Atmospheric Sciences*, 45(3), 439–462.

Yuval, J., Afargan, H., & Kaspi, Y. (2018). The relation between the seasonal changes in jet characteristics and the pacific midwinter minimum in eddy activity. *Geophysical Research Letters*, 45(18), 9995–10002.

Zhang, Y., & Held, I. M. (1999). A linear stochastic model of a GCM's midlatitude storm tracks. *Journal of the Atmospheric Sciences*, 56(19), 3416–3435.